JOURNAL OF BASIC SCIENCE AND ENGINEERING

PREPARATION, CHARACTERIZATION, AND CYTOTOXIC EVALUATION OF DOCETAXEL-LOADED POLYMERIC NANOPARTICLES USING NOVEL POLYMER SOLUPLUS® AS SURFACTANT

Sapana Shyamal Chaudhari [1*], Dr. Chainesh Shah[2], Dr. Shahzad Ahmed A. R[3]

[1] Research scholar in JJT University, Rajasthan.333010
[2] Professor and Vice Principal, Sigma University .390019
[3] Professor and Principal, JMCT Institute of pharmacy, Wadala road, Nashik, Maharashtra. 422006

DOI: https://doie.org/10.0126/Jbse.2025601255

Abstract: For better targeted delivery of docetaxel, the goal of this work was to create folate surface-engineered pegylated PLGA nanoparticles using Soluplus® as the only surfactant. The nanoparticles were created using a modified nanoprecipitation technique with Soluplus® as the surfactant. A variety of formulations' drug loading, zeta potential, particle size, polydispersity index, and entrapment efficiency were created and evaluated. Scanning electron microscopy was used to analyse and assess the nanoparticles' morphology. To find out if nanoparticles are more cytotoxic than free medicines, the MTT test was employed. As the nanoparticles were successfully fabricated, it was demonstrated that they outperformed free medicines in terms of cytotoxicity.

Keywords: Docetaxel, Nanoparticle, Anticancer, Soluplus®, Surfactant, Chemotherapy

Introduction:

The delivery of cytotoxic chemicals and drugs could change as a result of nanomedicine. The effectiveness of standard small molecule chemotherapies is limited, and their unintentional toxicities can worsen the condition of patientsNanoparticles are designed to alter the pharmacokinetic profiles and biodistribution of small molecule medications or contrast agents in patients in an attempt to improve imaging signals, reduce systemic toxicity, and/or increase therapeutic index. They also make it possible to deliver higher doses of these medications to the targeted tissue. Many clinically accessible nanomedicines, such as Doxil and Abraxane, as well as those undergoing clinical trials, have demonstrated improved treatment outcomes for a range of malignancies (Koziara et al., 2004, Spencer and Faulds, 1994).

Finding the ideal physicochemical characteristics that together provide molecular targeting, immunological evasion, and regulated drug release has proven to be a significant obstacle to the effective clinical translation of novel nanomedicines for the treatment of cancer. A comprehensive grasp of the complex interdependencies between these factors is necessary to improve the efficiency of nanoparticle dispersion to tumours (Sultan Alvi et al., 2017, Spencer and Faulds, 1994, Barbuti and Chen, 2015). Following treatment, people with triple-negative breast cancer typically have a worse prognosis than those with other subtypes of the disease. This result demonstrates the disease's innately bad outlook. Chemoresistance has been demonstrated in almost half of individuals with triple-negative breast cancer (Gluz et al., 2009). Engineered devices that can raise intracellular drug concentrations to the point where they overwhelm certain resistance pathways can be used to change the treatment resistance of triple-negative breast tumours (Gluz et al., 2009)(Lee and Foo, 2013, Panchagnula, 1998, Ma and Mumper, 2013, Skwarczynski et al., 2006, Long, 1994).

Vol. 22, No. 1, (2025)
ISSN: 1005-0930

In order to treat taxane-resistant triple-negative breast cancer, we have developed biodegradable nanoparticles that alter the pharmacokinetic profile of docetaxel and enhance its therapeutic index. It has been hypothesized that the performance of folate engineered pegylated PLGA-docetaxel nanoparticles was found to exhibit improved pharmacokinetic (PK) profiles, effectiveness, and tolerance that were significantly better than those of the therapeutic formulation of docetaxel. Using nanotechnology to administer docetaxel is one possible treatment strategy for triple-negative breast cancer (Linn et al., 2012)(Linn et al., 2012, Shamma and Basha, 2013). This present research work aimed to fabricate and evaluate folate surface engineered pegylated PLGA nanoparticles of Docetaxel for improved chemotherapy of cancer using Soluplus® as the sole surfactant. Surface shape, zeta potential, particle size, polydispersity index, drug loading and entrapment efficiency, and nanoparticles synthesised using Soluplus® as a surfactant were assessed subsequent to the evaluation of cytotoxicity.

Materials and Methods:

Drugs, chemicals and reagents:

PEG and PLGA were acquired from Himedia in Mumbai, India. Docetaxel was obtained from BASF (USA), while Soluplus® was a gift sample from Fresenius Kabi Oncology Limited. Only dependable and validated sources provided the remaining chemicals and reagents, which were all of analytical quality.

Investigation on Compatibility of Drug Excipients:

medicine degradation may result from interactions between the medicine and the excipients. For the dosage form to be stable and effective, the excipients must function effectively together. FTIR spectroscopy was used to investigate the possibility of drug interactions. The FTIR spectra of the drug and individual excipients (Bruker Instrument, Germany) were compared to the FTIR spectra of the drug and excipients' physical mixture over wave numbers ranging from 4000 cm-1 to 400 cm-1 in order to ascertain whether any interaction existed.

Synthesis of triple conjugate polymer (PPegF):

The triple conjugate polymer (PPegF) was synthesized with modifications based on literature. PLGA (50:50) was initially used to validate the process, followed by PLGA (75:25) for actual batches. PLGA (75:25) was dissolved in DCM, mixed with DCC and NHS (2:1:0.5), and reacted under nitrogen for 24 hours. The solution was dried and filtered. PEG-bisamine in DCM (1:2) was combined with activated PLGA in DCM and agitated under nitrogen for 12 hours. Ice-cold diethyl ether was used to precipitate the result, which was then filtered and dissolved in DMSO. FTIR and NMR confirmed the synthesis. Conjugation to Form PPegF, P-PEG was dissolved in DMSO with activated folic acid (DCC and NHS, 2:1:1) and reacted under nitrogen for 24 hours. Ice-cold methanol was used to precipitate the result, which was then filtered, dried, dissolved in DCM, centrifuged, and dried. The final product was validated by FTIR and NMR.

Formulation of nanoparticles:

To fabricate polymeric nanoparticles using a modified nanoprecipitation technique with solvent evaporation, a triblock copolymer composed of PLGA, PEG and Folate is used. First, 100 mg of the copolymer and the desired amount of a hydrophobic drug are dissolved in 10 mL of acetone, ensuring complete dissolution by stirring for 30 minutes. Meanwhile, a 1% (w/v) Soluplus® solution is prepared by dissolving Soluplus® in distilled water 50 mL, heating to 65°C while mixing until fully dissolved, and then cooling to room temperature. Then, using a syringe pump, the organic phase containing the medication and copolymer is gradually put to the aqueous solution of Soluplus® at 1 mL/min rate while being continuously stirred magnetically at 500 rpm. In this step, the organic solvent diffuses into the aqueous phase, causing the polymer to precipitate and form nanoparticles. By gradually eliminating the organic

solvent from the resulting nanoparticle suspension at 40°C under reduced pressure until all of the acetone has evaporated, a stable nanoparticle suspension is created. To pellet the nanoparticles and gather and purify them, the suspension is centrifuged for 25 minutes at 14,000 rpm. The particle is resuspended in distilled water after the supernatant is disposed of. To eliminate any remaining Soluplus® and unencapsulated medication, this washing procedure is carried out three times. Finally, the washed nanoparticle suspension is freeze-dried to obtain a dry powder by first freezing the suspension at -80°C and then lyophilizing it for 48 hours. The coding name for this initial formulation was SOLF1. Similar to SOLF1, SOLF2, SOLF3 and SOLF4 were also created with Soluplus® at different concentrations mentioned in the formulation composition table (Dian et al., 2014, Jog et al., 2016)(Dian et al., 2014, Jog et al., 2016).

Characterization of the nanoparticles:

Percentage Yield

Yields (%) of nanoparticle batches were computed using the following formula following their preparation modified nanoprecipitation method (Mukerjee and Vishwanatha, 2009):

$$Yield\ (\%) = \frac{\text{Weight (nanoparticles obtained)}}{\text{Weight (drug and polymer used for nanoparticles preparation)}} x100$$

Drug Loading and Entrapment Efficiency

To evaluate the drug loading and trapping effectiveness of the nanoparticles, two milligrams of docetaxel-loaded nanoparticles were meticulously weighed and put in a centrifuge tube with two milliliters of dichloromethane. The mixture was continually shaken at 37°C for three to four hours using a shaker incubator. Centrifugation was used to separate the continuous phase from the scattered phase. The drug's release was then determined by executing spectrophotometric measurements at 231 nm on the collected supernatant. The ratio of drug loading to entrapment efficiency was calculated using the following formulas: (Ling and Huang, 2008, Gupta et al., 2016):

$$Drug\ loading\ efficiency\ (\%) = \frac{\text{Quantity of Drug in Nanoparticles}}{\text{The amount of drug in nanoparticlescles}} x100$$

$$Entraapment\ efficiency\ (\%) = \frac{\text{Amount of drugs in nanoparticles}}{\text{Initial Drug Amount Added}} x100$$

Zeta Potential and Particle Size:

A solid-state laser was used to measure the particle size and size distribution of the nanoparticles using a Malvern Nano ZS90 equipped with a dynamic light scattering (DLS) system (Marsalek, 2014). A suitable amount of dried nanoparticles was suspended in double-distilled water and sonicated for a suitable duration prior to measurement. Next, the homogeneous suspension's average hydrodynamic particle size, size distribution, and polydispersity index were calculated. Zeta potential was also evaluated using the Malvern NANO ZS90. The ZP gives details on the long-term stability and particle surface charge. The dried nanoparticles in each formulation were suspended in double-distilled water and sonicated for the proper duration of time before measurement.

Scanning Electron Microscopy (SEM):

Scanning electron microscopy was used to examine the nanoparticles' form and surface properties using a Hitachi SEM, S-3600N (Radice et al., 2005). A suitable sample of nanoparticles was made by mounting a sample on metal stubs and using a razor blade to break it, with the assistance of Carbon tape with double-sided adhesive. The secondary electron emissive SEM was used to analyse the morphology of samples that had been sputter-coated with gold in an argon atmosphere.

Drug Release Study *in Vitro:*

In phosphate buffer (pH 7.4), the drug release from the produced nanoparticles was investigated. For drug release tests, Eppendorf tubes with 5 mg of freeze-dried nanoparticles and 2 ml of phosphate buffer were utilised. After that, the tubes were kept in an incubator at 37°C. Following zero, one, three, six, nine, twelve, twenty-four, thirty-six, and forty-eight hours of shaking at a rate of 130 revolutions per minute, we centrifuged the samples. The produced supernatant was then preserved in 0.5 millilitres. A fresh phosphate buffer solution was used in place of 0.5 millilitres of the extracted samples in order to maintain the same scenario or sink condition. Using a spectrophotometer, the amount of medication released from the samples was determined at 231 nm (Maji et al., 2014).

***In Vitro* Drug Release data and Pharmacokinetic modelling:**

Evaluating the kinetics of nanoparticles and the mechanism of drug release from them is crucial to comprehending their pharmacokinetic models. Numerous kinetic models, including zero order and first order models, were used to interpret data from in vitro drug release studies. Graphs were then created using the results of these equations. A regression analysis of the linear plots was performed to ascertain r2 and k, and the results were displayed (Jana et al., 2014).

Evaluation of cytotoxicity using the MTT assay:

Using the previously described MTT assay, the cytotoxicity of the free drugs and PPegF-NPs on breast cancer cells (MCF7) was assessed (Cao et al., 2016, Ahmed and Kaur, 2017, Lupu and Popescu, 2013).

Statistical analysis:

Data is presented as mean ± SD. The data was post-hocly analysed using the Tukey-Kramer test and one-way ANOVA, with a $p < 0.05$ limit for statistical differences between the groups. This study made use of GraphPad Prism (Version 8.01, GraphPad Software, San Diego, USA).

Results and Discussion:

Drug-excipient compatibility studies:

The FTIR spectra of PLGA, PEG, Docetaxel, and Soluplus®, when compared to the PLGA-PEG-Docetaxel-Soluplus® physical mixture, clearly showed that the drug and the excipients were found to retain their major and characteristic peaks. This implied that the excipients are completely stable and incompatible with one another.

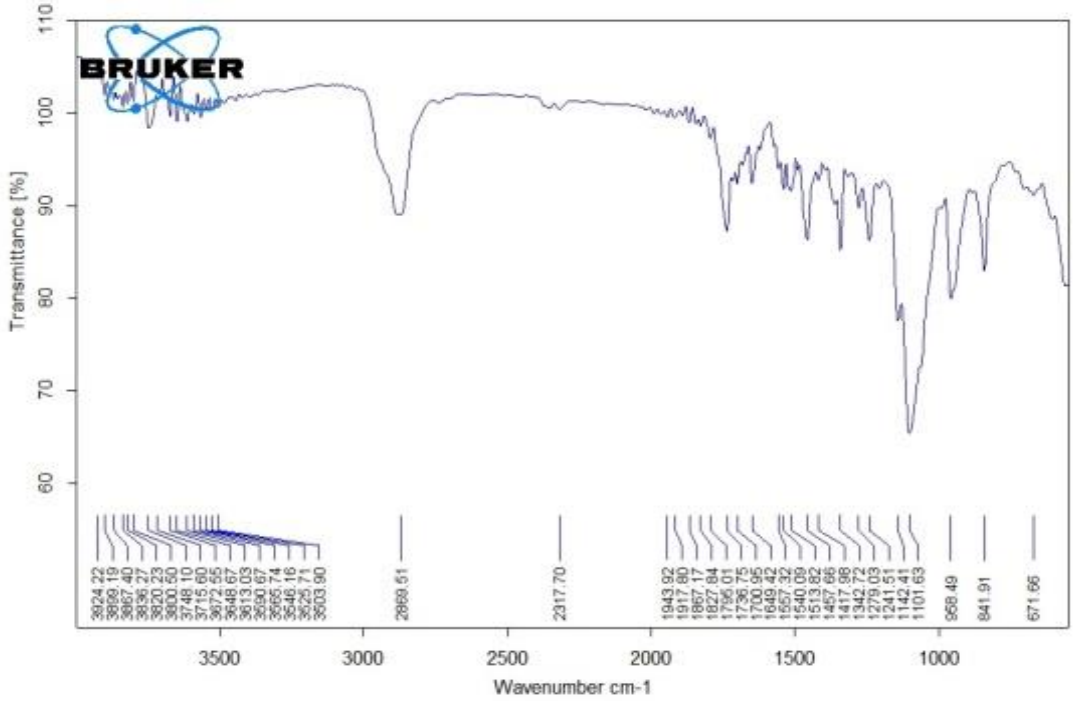

Figure 1. Physical combination FTIR spectra of Soluplus®, PLGA, PEG, and Docetaxel.

Nanoparticle preparation:

The synthesis of docetaxel-loaded nanoparticles for this investigation was done using a modified nanoprecipitation technique. As indicated in Table 1, the technique was nanoprecipitation technique modified accordingly. This method can be used to create formulations with the required surface, encapsulation, and size characteristics. Even when other stabilisers are also utilised, PVA is commonly used as a stabiliser. Instead of using PVA in this experiment, Soluplus® was used. Table 1 displayed the composition of the nanoformulations using the modified processes.

Table 1: compositions of the nanoparticles (SOLF1–SOLF4) and their yield %

Formulation	PPegF (mg)	Docetaxel (mg)	Organic Solvent (mL)	Stabilizer cum Surfactant (Soluplus®) Concentration (%)	Aqueous Phase Volume (mL)
SOLF1	20	10	10	0.5	25
SOLF2	20	10	10	1.0	50
SOLF3	20	10	15	1.5	75
SOLF4	20	10	10	2.0	100

Characterization of the polymeric nanoparticles:

SEM images of smooth-surfaced nanoparticles were shown in Figure 2. Table 2 demonstrated the homogenous distribution of submicron-sized Docetaxel-loaded nanoparticles under experimental settings, as determined by the evaluation of its polydispersity index.

Vol. 22, No. 1, (2025)
ISSN: 1005-0930

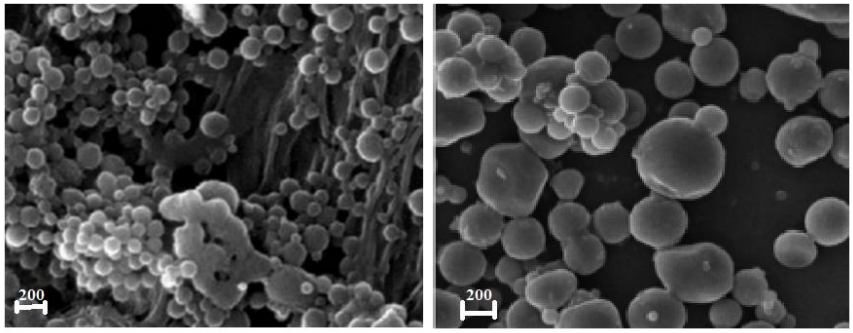

Figure 2. Prepared PLGA nanoparticles as seen in the SEM images (SOLF4)

The effectiveness and safety of therapeutic materials can be adversely affected by a number of problems, including inadequate drug transport to the targeted tissue or undesired side effects, including severe toxicities in healthy tissue and organs. Encapsulating a drug in nanocarriers with definite and reliable properties can result in improved bioavailability and diminished side effects. The physicochemical characteristics of nanocarriers, such as the distribution of particle sizes within the nanocarrier, determine their migration to cluster in the target tissue. Therefore, to deliver safe, stable, and effective nanocarriers, homogenous (monodisperse) populations of nanocarriers of a specific size must be manufactured homogeneously.

Table 2: Characteristics of Polymeric Nanoparticles Loaded with Docetaxel and fabricated with Surfactant Soluplus®

Formulation code	Particle size (nm)	Polydispersity index (PDI)	Zeta potential (mV)	Drug loading (%)	Entrapment efficiency (%)
				(Mean ± SD) *	
SOLF1	387.50	0.811	-23.6	16.77 ±0.10	37.25±0.76
SOLF2	334.29	0.887	-18.9	16.28±0.46	36.43±0.77
SOLF3	433.50	0.915	-19.5	17.63 ±0.52	33.63±0.61
SOLF4	304.64	1.000	-16.9	19.09 ± 0.51	37.17±0.58

Nonetheless, it's interesting to regulate the distribution of particle sizes without taking into account the chemical makeup of the nanocarriers or the kinds of solvents and cosolvents used in their creation (Mozafari et al., 2017, Bulbake et al., 2017). The current investigation indicated that all PDI values were greater than 0.7, indicating wide particle size distribution. To establish if the formulations are adequate, more research is required. Zeta potential, particle size, and PDI (almost 0.7) demonstrated that formulation SOLF4 had a noticeably better profile than the other nanoformulations. A zeta potential (ZP) evaluation of docetaxel-loaded nanoparticles was performed in order to ascertain the surface charge of the particles. The zeta potential has an impact on the biodistribution of nanoparticles in addition to their pharmacokinetics and biodistribution in the physiological environment. It has been shown that negatively charged nanoemulsions are more readily absorbed by the reticuloendothelial system and eliminated more rapidly than positively or neutrally charged nanoparticles (Xu, 2008). Additionally, the zeta potential of the nanoparticles and the type of binding that takes place between the pharmaceuticals and the nanoparticles reflect the effectiveness of drug loading and the rate at which drugs can be resorbable from the nanoparticles. It can also be utilised to ascertain whether the drug or active ingredient is contained at the core of the nanoparticles or, if so, whether adsorption occurs on their surface. Studies on negatively

charged nanoparticles reveal that they stay in the bloodstream longer and are removed from it more slowly than their positively charged counterparts following injection (Honary and Zahir, 2013). Additionally, research has shown that cationic charges or negative zeta potentials make nanoparticles more harmful. This might be because the nanoparticles and the negatively charged cell membrane are making more contact, which might lead to the membrane becoming unstable or even disintegrating (Honary and Zahir, 2013). Additionally, it was discovered that every formulation had polymeric nanoparticle ZP values, a sign of stability. According to the zeta potential profiles of PPegF-NPs including Soluplus® as a surface active agent, these particles may offer a sustainable way to encapsulate hydrophobic medications such as docetaxel. Although Soluplus® is a good surface-active agent, it wasn't the ideal choice for producing PPegF-NPs in this specific investigation, according to the data taken into account. For greater stability of the nanoparticles, further research may be able to expand the particle size distribution and enhance the particle size.

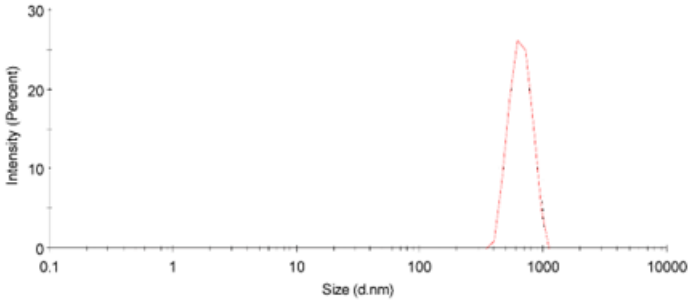

Figure 3. SOLF1 particle size distribution curve

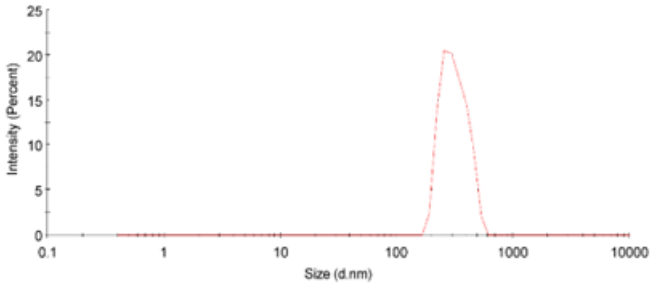

Figure 4. SOLF2 particle size distribution curve

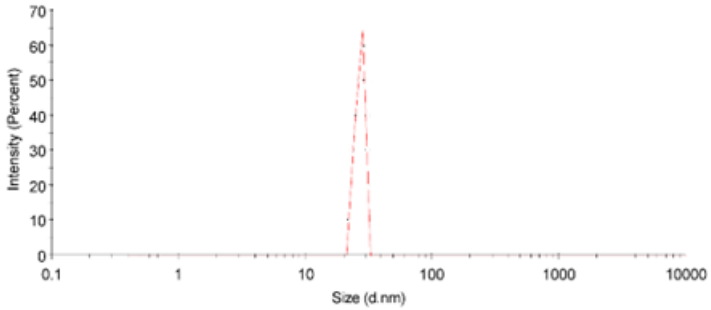

Figure 5. SOLF3 particle size distribution curve

Vol. 22, No. 1, (2025)
ISSN: 1005-0930

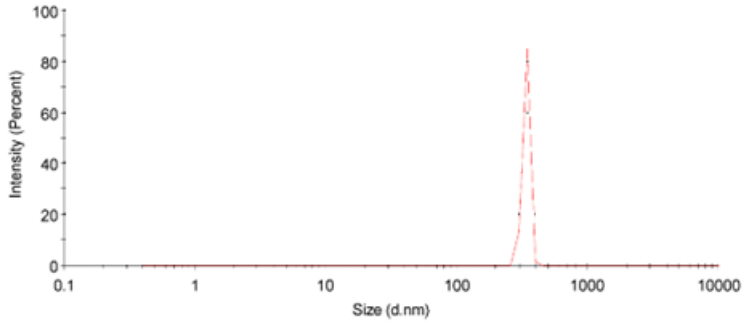

Figure 6. Particle size distribution curve for SOLF4

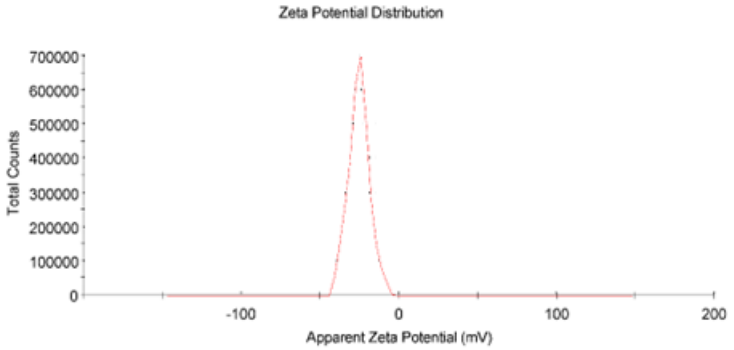

Figure 7. SOLF1's zeta potential

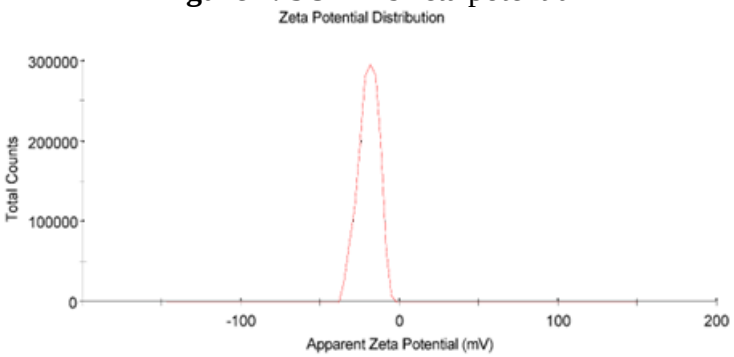

Figure 8. SOLF2's zeta potential

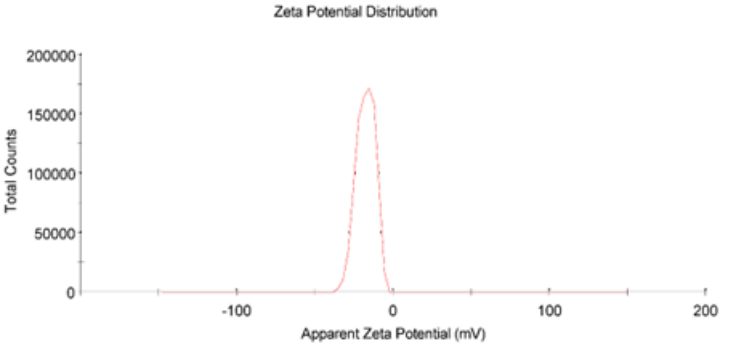

Figure 9. SOLF3's zeta potential

Vol. 22, No. 1, (2025)
ISSN: 1005-0930

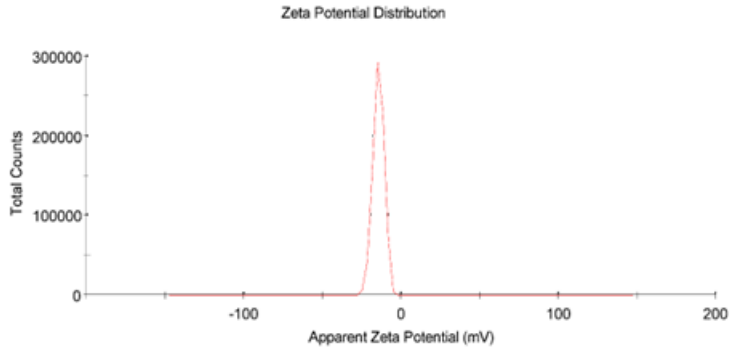

Figure 10. SOLF4's zeta potential

Evaluation of entrapment efficiency and drug loading:

Drug loading values estimated and calculated are 16.77 ± 0.10%, 19.09 ± 0.51%, 17.63 ± 0.52% and 16.28 ± 0.46% for SOLF1, SOLF2, SOLF3, and SOLF4, respectively. Among these, SOLF2 demonstrated the maximum drug loading at 19.09 ± 0.51%, while SOLF4 had the lowest drug loading at 16.28 ± 0.46%. The estimated and calculated entrapment efficiency values are 37.25 ± 0.76%, 37.17 ± 0.58%, 33.63 ± 0.61% and 36.43 ± 0.77% for SOLF1, SOLF2, SOLF3, and for SOLF4, respectively. SOLF1 demonstrated the highest entrapment efficiency at 37.25 ± 0.76%, indicating it is the most effective at encapsulating the drug, while SOLF3 had the lowest entrapment efficiency at 33.63 ± 0.61%. Comparatively, SOLF1 exhibited a good balance with moderate drug loading and the highest entrapment efficiency, indicating SOLF1 a effective and strong candidate for effective drug delivery. However, even at this highest drug loading of SOLF2 the encapsulation efficiency is a little lower compared to that of SOLF1 but still very high and therefore it can be used in any formulation where a higher content of drug needs to be contained. Drug loading in SOLF3 was found to be moderate but entrapment efficiency the lowest of all the formulations, demonstrating a likely drawback during encapsulation process (Table 2). SOLF4 exhibited the least drug loading while its entrapment efficiency to a certain extent showed promise for enhanced drug content without compromising their encapsulating ability. Overall, it was found that SOLF1 was the most balanced when taking into account both drug loading and entrapment efficiency, while SOLF2 had a larger drug loading. SOLF3's entrapment efficiency was discovered to be optimal. This inference is of key prominence for the design and optimization of novel formulations with ideal balance between drug loading and entrapment efficiency leading to efficient drug delivery. A number of factors need to be considered in order to guarantee the efficacy of this formulation and nanoparticle creation process, including the kind and concentration of the stabiliser, the rate at which homogenisation takes place, and the optimal ratio of the medicine to the polymer utilised (Maji et al., 2014).

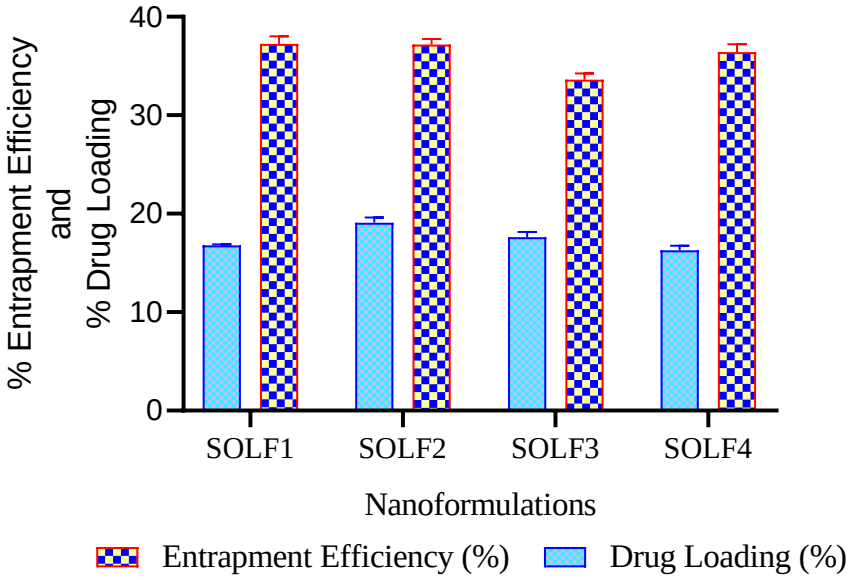

Figure 14. Drug loading and entrapment effectiveness of SOLF1–SOLF4 nanoformulations.

In vitro drug release and pharmacokinetic modelling and of PPegF-NPs nanoparticles loaded with docetaxel:

For all formulations, the in vitro drug release at 1 hour ranged from 12.573 ± 0.073 to 16.013 ± 0.029, and at 3 hours, it ranged from 34.023 ± 0.053 to 41.723 ± 0.079. According to this data, rather of increasing suddenly during the first three hours of the study, the drug release increases steadily. The encapsulating material's degradation may be the cause of the first phase, which is followed by a steady diffusion that, after 48 hours, reached 68.853 ± 0.059% for SOLF4. SOLF4 had the highest drug release at 48 hours, with a measurement of 68.853 ± 0.059%. When the linearity of the kinetic pattern of this in vitro drug release was examined, zero-order kinetics were shown by the computed R2 values. This was followed by very good linearity in the Korsmeyer-Peppas plot. The release behaviour of the polymeric formulation based on the in vitro data is validated by thorough kinetic modelling of the in vitro release data using the Korsmeyer-Peppas model, which depicts its release mechanism. An 'n' number was also displayed by SOLF4, the formulation with the biggest release, indicating that 'Fickian diffusion' was the mechanism behind its release. This discovery unequivocally shows that medicines are released from these polymeric structures via a diffusion-based zero-order process. The different rate constants and exponents derived from drug release data using multiple kinetic models are contrasted in the following table 3. As a result, this study unequivocally shows that a zero-order mechanism involving diffusion releases medicines from polymeric structures. The several rate constants and exponents that have been computed from drug release data using multiple kinetic models are contrasted in the following table 3.

Vol. 22, No. 1, (2025)
ISSN: 1005-0930

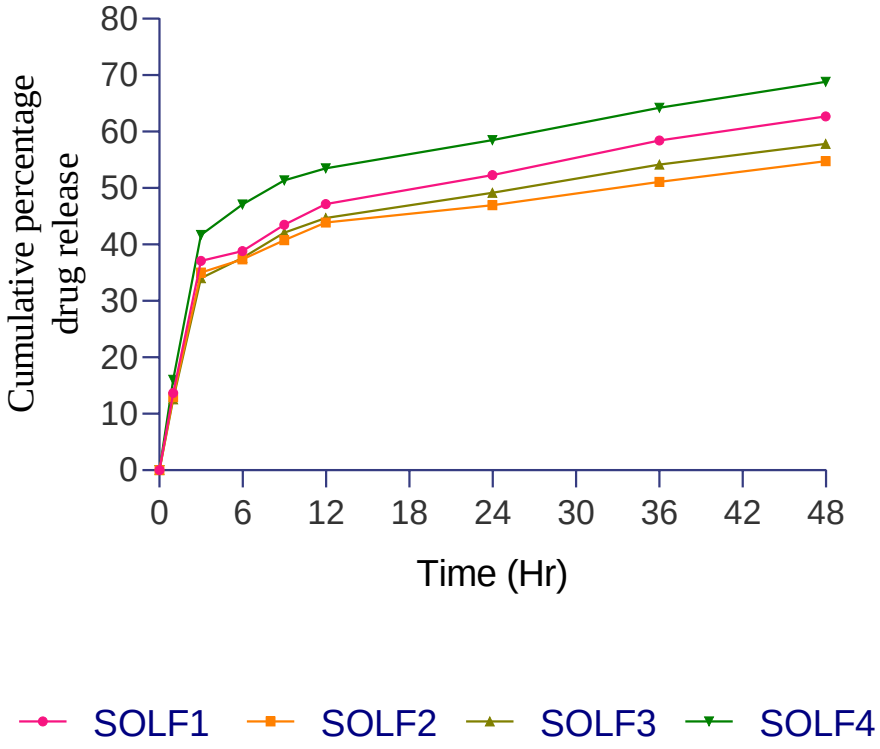

Figure 15. Cumulative percentage of drugs released plotted against time

Table 3: Data on drug release in vitro using several kinetic models

Formulation Code	Zero Order Model	First Order Model	Higuchi Model	Hixon-Crowell Model	Korsmeyer-Peppas Model	
	R^2_Z	R^2_F	R^2_H	R^2_{HC}	R^2_{KP}	n
SOLF1	0.982	0.975	0.993	0.989	0.998	0.502
SOLF2	0.978	0.970	0.991	0.986	0.996	0.488
SOLF3	0.974	0.965	0.990	0.983	0.995	0.491
SOLF4	0.987	0.982	0.996	0.992	0.999	0.526

Evaluation of cytotoxicity using MTT assay:

To find SOLF4's IC 50 (50% growth inhibition) against MCF7 cells at various doses, an MTT test was used. Figure 16 displays the results of the studies, which used various amounts of SOLF4. Comparing SOLF4 dosages ranging from 100 nM to 2000 nM to control and free drug concentrations revealed significant impacts on MCF7 cells in MTT experiments. At the SOLF4 concentration that demonstrated the maximum cytotoxicity against the MCF7 cell, 2000 nM, cell viability was 11.87±0.99 percent. As SOLF4 concentration rose, the growth inhibition percentage rose as well, and the assay's IC 50 value was 105 µg/ml. In contrast to the formulation of free medication. Significant cytotoxicity was shown by SOLF4, proving the Nanoformulation's advantage over free drug.

Vol. 22, No. 1, (2025)
ISSN: 1005-0930

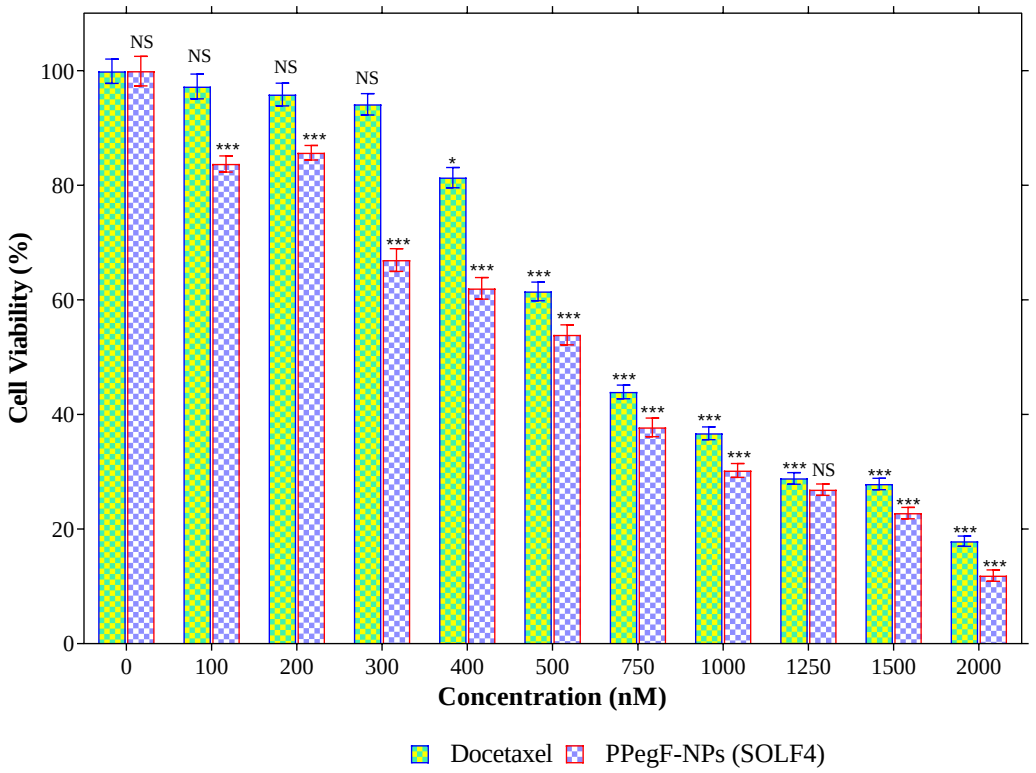

Figure 16. Evaluation of cytotoxicity of the PPegF-NPs (SOLF4) nanoparticles as compared to free drug

Conclusion:

The physicochemical characteristics of PPegF nanoparticles loaded with docetaxel that were made using the modified nanoprecipitation techniques with solvent evaporation techniques was evaluated in this work. The optimal formulation was found to be (SOLF4) after characterisation. Using SEM, the morphological characteristics of the chosen formulation were examined in more detail. The SEM images showed many spherical polymeric nanoparticles. The lyophilized polymeric nanoparticles loaded with docetaxel in formulation SOLF4 released a cumulative amount of docetaxel that was more than that released by the formulations used in comparison. In vitro research on the drug release kinetics for formulation SOLF4 revealed better linear R2 values (0.978) and zero order kinetics (0.977) in the Korsmeyer-Peppas plot. "Fickian diffusion" from matrix-type nanoparticles is indicated by a drug release exponent (n value) on the Korsmeyer-Peppas plot that is less than 0.5. The best and most efficient formulation was determined by in vitro drug release experiments to be SOLF4. Therefore, using PPegF-NPs to deliver docetaxel may be a promising and successful way to treat cancer. Using Soluplus® as a surfactant, docetaxel nanoparticles were effectively created and assessed. With the correct loading, encapsulation, size, and shape, Soluplus® has demonstrated its effectiveness as a surfactant and has the potential to be a valuable vehicle for encapsulating and delivering poorly water-soluble compounds as nanoparticles. To ascertain whether Soluplus® can be utilised as the sole surfactant in the production of nanoparticles in a feasible and efficient manner, more investigation is necessary.

Reference:

AHMED, S. & KAUR, K. 2017. Design, synthesis, and validation of an *in vitro* platform peptide-whole cell screening assay using MTT reagent. *Journal of Taibah University for Science*, 11**,** 487-496.

BARBUTI, A. M. & CHEN, Z.-S. 2015. Paclitaxel through the ages of anticancer therapy: exploring its role in chemoresistance and radiation therapy. *Cancers,* 7**,** 2360-2371.

BULBAKE, U., DOPPALAPUDI, S., KOMMINENI, N. & KHAN, W. 2017. Liposomal formulations in clinical use: an updated review. *Pharmaceutics,* 9**,** 12.

CAO, L.-B., ZENG, S. & ZHAO, W. 2016. Highly Stable PEGylated Poly(lactic-coglycolic acid) (PLGA) Nanoparticles for the Effective Delivery of Docetaxel in Prostate Cancers. *Nanoscale Research Letters,* 11**,** 1-9.

DIAN, L., YU, E., CHEN, X., WEN, X., ZHANG, Z., QIN, L., WANG, Q., LI, G. & WU, C. 2014. Enhancing oral bioavailability of quercetin using novel soluplus polymeric micelles. *Nanoscale Res Lett,* 9**,** 2406.

GLUZ, O., LIEDTKE, C., GOTTSCHALK, N., PUSZTAI, L., NITZ, U. & HARBECK, N. 2009. Triple-negative breast cancer--current status and future directions. *Ann Oncol,* 20**,** 1913-27.

GUPTA, A., KAUR, C. D., SARAF, S. & SARAF, S. 2016. Formulation, characterization, and evaluation of ligand-conjugated biodegradable quercetin nanoparticles for active targeting. *Artif Cells Nanomed Biotechnol,* 44**,** 960-70.

HONARY, S. & ZAHIR, F. 2013. Effect of zeta potential on the properties of nano-drug delivery systems-a review (Part 1). *Tropical Journal of Pharmaceutical Research,* 12**,** 255-264.

HONARY, S. & ZAHIR, F. 2013 Effect of Zeta Potential on the Properties of Nano-Drug Delivery Systems - A Review (Part 2). *Tropical Journal of Pharmaceutical Research,* 12.

JANA, U., MOHANTY, A. K., PAL, S. L., MANNA, P. K. & MOHANTA, G. P. 2014. Felodipine loaded PLGA nanoparticles: preparation, physicochemical characterization and in vivo toxicity study. *Nano Convergence,* 1**,** 31.

JOG, R., KUMAR, S., SHEN, J., JUGADE, N., TAN, D. C., GOKHALE, R. & BURGESS, D. J. 2016. Formulation design and evaluation of amorphous ABT-102 nanoparticles. *Int J Pharm,* 498**,** 153-69.

KOZIARA, J. M., LOCKMAN, P. R., ALLEN, D. D. & MUMPER, R. J. 2004. Paclitaxel nanoparticles for the potential treatment of brain tumors. *Journal of controlled release,* 99**,** 259-269.

LEE, L. K. & FOO, K. Y. 2013. An appraisal of the therapeutic value of lycopene for the chemoprevention of prostate cancer: A nutrigenomic approach. *Food Research International,* 54**,** 1217-1228.

LING, Y. & HUANG, Y. 2008. Preparation and Release Efficiency of Poly (lactic-co-glycolic) Acid Nanoparticles for Drug Loaded Paclitaxel. *In:* PENG, Y. & WENG, X. (eds.) *7th Asian-Pacific Conference on Medical and Biological Engineering: APCMBE 2008 22–25 April 2008 Beijing, China.* Berlin, Heidelberg: Springer Berlin Heidelberg.

LINN, M., COLLNOT, E.-M., DJURIC, D., HEMPEL, K., FABIAN, E., KOLTER, K. & LEHR, C.-M. 2012. Soluplus® as an effective absorption enhancer of poorly soluble drugs in vitro and in vivo. *European Journal of Pharmaceutical Sciences,* 45**,** 336-343.

LONG, H. J. Paclitaxel (Taxol): a novel anticancer chemotherapeutic drug. Mayo Clinic Proceedings, 1994. Elsevier, 341-345.

LUPU, A. R. & POPESCU, T. 2013. The noncellular reduction of MTT tetrazolium salt by TiO(2) nanoparticles and its implications for cytotoxicity assays. *Toxicol In Vitro,* 27**,** 1445-50.

MA, P. & MUMPER, R. J. 2013. Paclitaxel Nano-Delivery Systems: A Comprehensive Review. *J Nanomed Nanotechnol,* 4**,** 1000164.

MAJI, R., DEY, N. S., SATAPATHY, B. S., MUKHERJEE, B. & MONDAL, S. 2014. Preparation and characterization of Tamoxifen citrate loaded nanoparticles for breast cancer therapy. *International journal of nanomedicine,* 9**,** 3107.

MARSALEK, R. 2014. Particle size and zeta potential of ZnO. *APCBEE procedia,* 9**,** 13-17.

MOZAFARI, M., DANAEI, M., JAVANMARD, R., RAJI, M. & MAHERANI, B. 2017. Nanoscale lipidic carrier systems: importance of preparation method and solvents. Glob. *J. Nano,* 2.

MUKERJEE, A. & VISHWANATHA, J. K. 2009. Formulation, characterization and evaluation of curcumin-loaded PLGA nanospheres for cancer therapy. *Anticancer Res,* 29**,** 3867-75.

PANCHAGNULA, R. 1998. Pharmaceutical aspects of paclitaxel. *International Journal of Pharmaceutics,* 172**,** 1-15.

RADICE, S., KERN, P., MICHLER, J. & TEXTOR, M. 2005. Bioactive Coatings for Implants by Electrophoretic Deposition. *European Cells Materials,* 10**,** 5.

SHAMMA, R. N. & BASHA, M. 2013. Soluplus®: a novel polymeric solubilizer for optimization of carvedilol solid dispersions: formulation design and effect of method of preparation. *Powder technology,* 237**,** 406-414.

SKWARCZYNSKI, M., HAYASHI, Y. & KISO, Y. 2006. Paclitaxel prodrugs: toward smarter delivery of anticancer agents. *Journal of medicinal chemistry,* 49**,** 7253-7269.

SPENCER, C. M. & FAULDS, D. 1994. Paclitaxel. *Drugs,* 48**,** 794-847.

SULTAN ALVI, S., ANSARI, I. A., KHAN, I., IQBAL, J. & KHAN, M. S. 2017. Potential role of lycopene in targeting proprotein convertase subtilisin/kexin type-9 to combat hypercholesterolemia. *Free Radic Biol Med,* 108**,** 394-403.

XU, R. 2008. Progress in nanoparticles characterization: Sizing and zeta potential measurement. *Particuology,* 6**,** 112-115.